Supplementary Note 1

Comparison of TERC systems with other electrochemical thermoelectric conversion systems:

The basic principle of thermally regenerative battery (TRB) is the combination of traditional thermal separation technology and electrochemical cells, that is, free energy change is generated through thermal separation technology, which is used in electrochemical cells to achieve the conversion of low temperature heat energy to electric energy. Further, TRB can be divided into thermally regenerative amino battery (TRAB) based on complex reaction power generation and thermal separation-salt difference power generation technology, which use chemical free energy and mixing free energy respectively in the discharge process. Thermo-electrochemical cell (TEC) operates based on seebeck coefficient under non-isothermal conditions, converting heat into electricity energy by electrochemical battery. Thermally regenerative electrochemical cycle (TREC) utilizes the temperature dependence of the electrode potential to achieve the conversion of heat to electricity energy through the cycle operation of heating, charging, cooling and discharging.

From the aspects of absolute efficiency, relative efficiency, and power density, a comprehensive comparative evaluation of each system is conducted. Specifically, absolute efficiency, defined as the ratio of output work to input heat energy, represents the heat to electricity conversion performance of the system. Relative efficiency measures the system's efficiency relative to the Carnot cycle at a given operating temperature, calculated as the ratio of absolute efficiency to Carnot efficiency. The power density reflects the output power of the system. The assessment of three metrics provides a comprehensive understanding of the strengths and limitations of each system.

As evident from the graphical representation, TREC exhibits the highest absolute and relative efficiencies among the three systems, yet possesses the lowest output power density. This underscores the criticality of exploring higher power density in TREC. Conversely, TRAB boasts the highest output power density, albeit with comparatively lower absolute and relative efficiencies. Hence, enhancing its efficiency is a pivotal step towards improving its overall performance. Thermally regenerative cell based on thermal separation-salt difference power generation technology exhibits high power density and relative efficiency, but are limited by the distillation characteristics, which require a high temperature (>85°C) for thermal energy. TEC demonstrates a power density that surpasses TREC, while absolute and relative efficiencies are comparable to TRB. TEC enjoys a broad application spectrum, having been studied across temperature difference from 10°C to 90°C. It is noteworthy that the data pertaining to the EBC system are derived from theoretical calculations, rather than experimental data, thus precluding a direct comparative analysis.

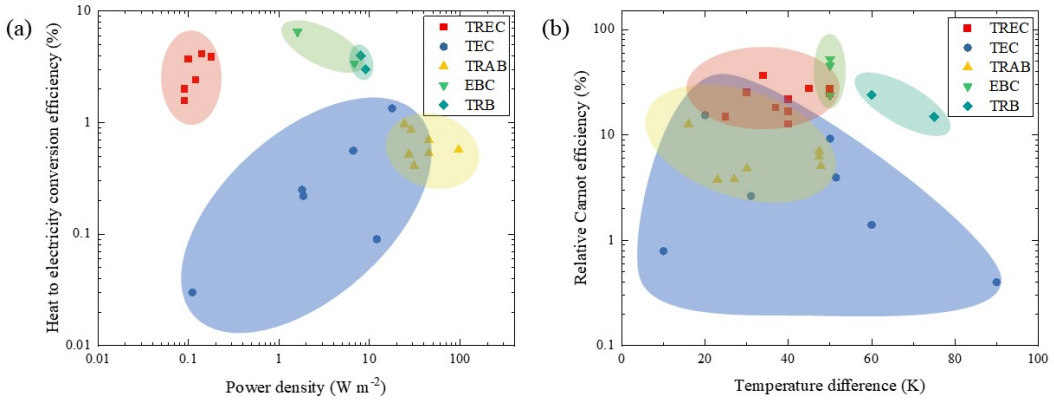

Fig. S1 Comparison of several electrochemical heat to electricity conversion systems from (a)

power density, heat to electricity conversion efficiency, and (b) relative Carnot efficiency

Supplementary Note 2

In order to compare this study with existing studies, key parameters such as redox pairs, temperature coefficient, operating temperature, efficiency, etc. are summarized in Table S1.

Table. S1 Experimental performance of TREC

Year	Authors	Redox pairs	Temperature coefficient	Operating temperature	Temperature difference	Absolute efficiency	Relative efficiency	Type
2014	Lee S W, et al.[14]	CuHCFe; Cu/Cu^{2+}	-1.2 mV/K	10℃-60℃	50℃	3.70%	24.65%	electrode
2014	Yang Y et al.[15]	NiHCF; Ag/AgCl	-0.74 mV/K	15℃-55℃	40℃	1.60%	13.13%	membrane
2014	Yang Y et al.[16]	$Fe(CN)_6^{3-/4-}$; $KFe^{II}Fe^{III}(CN)_6$	-1.45 mV/K	20℃-60℃	40℃	2.00%	16.65%	charging-free
2021	Cheng C et al.[18]	NiHCF(K^+); Zn/Zn^{2+}	-2.27 mV/K	10℃-40℃	30℃	2.41%	25.15%	electrode
2021	Gao C et al.[21]	CuHCFe; $Cu/Cu^{2+}(Rb^+)$	-1.004 mV/K	10℃-50℃	40℃	4.34%	35.06%	electrolyte
2022	Jung S et al.[20]	MnHCF; Ag/AgCl	-0.72 mV/K	15℃-55℃	40℃	5.17%	42.41%	electrode
2022	Huo D et al.[23]	CuHCFe; $Cu/Cu^{2+}(Na^+/K^+)$	-1.38 mV/K	12℃-46℃	34℃	3.90%	36.40%	electrolyte
2023	Zhang H et al.[17]	$Li_3Fe(CN)_6$/ $Li_4Fe(CN)_6$; LFP/FP	-2 mV/K	21.5℃-51.5℃	30℃	1.81%	19.91%	charging-free
2023	Li X et al.[24]	CuHCFe; $Fe^{2+/3+}$(ClO_4^-)	-3.04 mV/K	10℃-60℃	50℃	4.1%	27%	electrolyte
2023	Wu A et al.[25]	NaTFSI/HbetTFSI/H_2O; CuHCFe	-1.5 mV/K	10℃-30℃	20℃	1.32%	20.00%	electrolyte
2024	This study	VO_2^+/VO^{2+}; V^{2+}/V^{3+}	-1.4 mV/K	10℃-40℃	30℃	2.54%*	-	-

In the table, * represents the normalized thermal efficiency obtained in this study, and both the heat to electricity conversion efficiency reflect heat to electricity conversion performance of the system.

Supplementary Note 3

Three important metrics:

Efficiency is an important criterion for evaluating VRFB performance, which can be expressed in a variety of ways. In evaluating the performance of a VRFB, the following metrics are often used: coulombic efficiency (CE), voltage efficiency (VE), and energy efficiency (EE). The coulombic efficiency is the ratio of discharge capacity to the charge capacity of VRFB. The voltage efficiency can be calculated by dividing the average discharge voltage by the average charge voltage. The definition of energy efficiency is the ratio of the energy that is discharged to the required charge energy for VRFB. These quantities are defined as follows:

$$CE = \frac{\int_0^{t_d} i_d dt}{\int_0^{t_c} i_c dt} \tag{1}$$

$$VE = \frac{\int_0^{t_d} V_d dt}{\int_0^{t_c} V_c dt} \tag{2}$$

$$EE = \frac{\int_0^{t_d} P_d dt}{\int_0^{t_c} P_c dt} = CE \times VE \tag{3}$$

Thermoelectric conversion efficiency:

The thermoelectric conversion efficiency reflects the conversion degree of heat energy to electric energy, and is the ratio of output network to input heat energy. The calculation formula η_{TREC} for the efficiency of TREC system is given:[14]

$$\eta_{TREC} = \frac{W}{Q_H + Q_{HR}} \tag{4}$$

Where W is the net work output in one cycle, The energy input to complete the cycle consists of two parts: the heat absorbed at heat source Q_H and the external heat required to heat the system up Q_{HR}. W can be expressed as

$$W = W_{\max} - E_{loss} = \Delta T \Delta S - E_{loss} \tag{5}$$

Where $\Delta T \Delta S$ is the maximum output work of the system, and E_{loss} is the energy lost by the system due to factors such as battery resistance. Q_H can be expressed as

$$Q_H = T_H (S_{\mathrm{ch},H} - S_{\mathrm{dis},H}) = T_H \Delta S \tag{6}$$

For Q_{HR}, as a part of heat rejected in the cooling process can be used to heat the system up through a heat recuperation system, the external energy needed in the heating process is

The energy input to complete the cycle consists of two parts: the heat absorbed at heat source ($Q_H = T_H \Delta S$) and the external heat required to raise the system temperature ($Q_{HR} = C_p \Delta T$).

$$Q_{HR} = (1 - \eta_{HX}) C_p \Delta T \tag{7}$$

Where C_p is specific heat, η_{HX} is regenerative efficiency. In addition, $\Delta T \Delta S = \Delta T \alpha_{cell} q_c$, q_c is the charge capacity of the battery. So η_{TREC} can be simplified as

$$\eta_{TREC} = \frac{\Delta T \Delta S - E_{loss}}{T_H \Delta S + (1 - \eta_{HR}) C_p \Delta T} \tag{8}$$

However, since the energy lost by the all-vanadium flow battery itself may be greater than the energy gained by the TREC, the η_{TREC} is less than 0 possibly. Therefore, without considering reheating, the normalized thermal efficiency of the integrated system is defined as:

$$\eta_{\text{sys}} = \frac{(U_{D,TREC} - U_{C,TREC}) - (U_{D,T_{Ref}} - U_{C,T_{Ref}})}{T_H \alpha_{cell} q_c + C_p \Delta T} \tag{9}$$

Where $U_{D,TREC}$ is discharge energy of TREC system, $U_{C,TREC}$ is charging energy of TREC system; $U_{D,TRef}$ is the discharge energy at the reference temperature; $U_{C,TRef}$ are charging energy at reference temperature; T_{Ref} is the reference temperature. The η_{sys} considers the energy gained from the thermodynamic cycle relative to the isothermal cycle at the reference temperature.

Supplementary Note 4

Experimental system specific devices introduction：

The specific device of the experimental system is shown in the Fig. S2. The experimental system consists of the following components: electrochemical workstation, the flow battery unit, two electrolyte reservoirs, two peristaltic pumps, some connecting fittings, a data acquisition instrument, platinum thermal resistance, two heater bands and a thermostat water bath. Technical parameters of the graphite felt electrode are shown in Table. S2. Technical parameters of ion exchange membrane are shown in Table. S3.

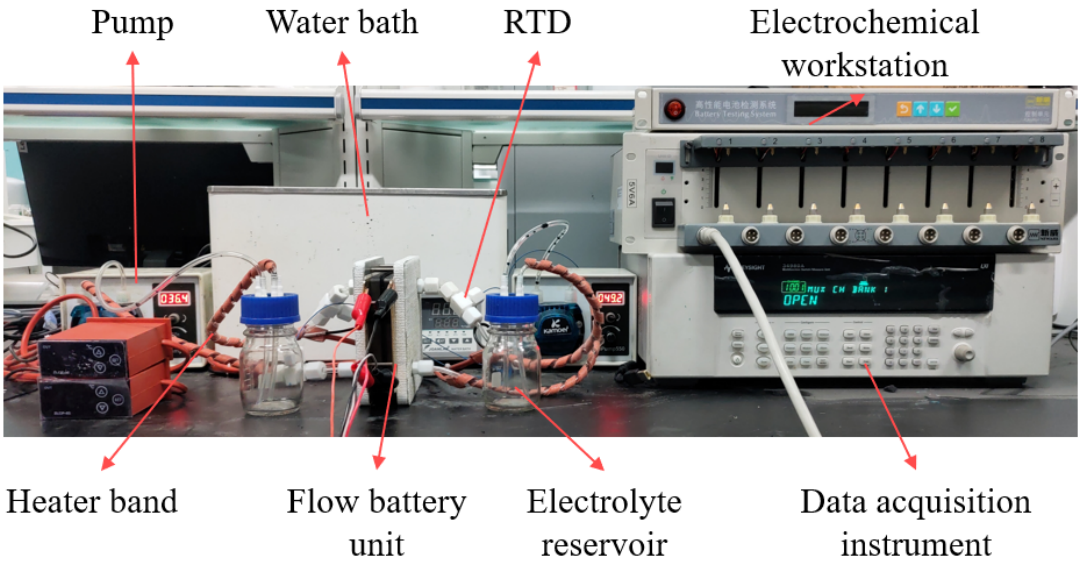

Fig. S2 Diagram of experimental system specific devices

Table. S2 Parameters of graphite felt electrode

Parameters	Technical parameters
Carbon content (%)	≥99%
Heat conductivity coefficient (w $m^{-1}K^{-1}$)	0.25
Strength of extension (MPa)	0.41
Capacity (g cm^{-3})	0.09±0.02
Ash content (%)	≤0.06
Thickness (mm)	4.35±7.5%
Length (mm)	8
Width (mm)	8

Table. S3 Parameter of ion exchange membrane

	Technical parameters
Brand	Dupont
Model number	Nafion-212
Thickness (μm)	50
Density (g m^{-3})	100
Electric conductivity (S cm^{-3})	0.083

Supplementary Note 5

Measurement of temperature coefficient of half-cell reaction：

Referencing the experimental method of Rajan et al shown in Fig. S3(a), the temperature coefficient of half-cell is tested as follows:

The electrolyte of the same state is passed on both sides of the battery, such as an anode electrolyte with SOC of 0.5, the electrolyte on one side is placed in a constant temperature water bath, and the temperature of the electrolyte on the other side is changed. As the temperature changes, the electrode potential changes. The thermal resistance is used to monitor the temperature of the electrolyte and calculate the temperature difference between the two sides. The temperature coefficient of anode and cathode electrolyte was obtained by recording the voltage of battery under different temperature difference. The temperature coefficients of half cells under different SOCs are shown in Figure. S3. When SOC is 0.3, the temperature coefficients of positive and negative electrodes are -0.20 mV K^{-1} and 1.18 mV K^{-1}. When SOC is 0.5, the temperature coefficients of positive and negative electrodes are -0.21 mV K^{-1} and 1.21 mV K^{-1}. When SOC is 0.7, the temperature coefficients of positive and negative electrodes are -0.20 mV K^{-1} and 1.16 mV K^{-1}. The experimental results show that the full temperature coefficient of the cell is effective.

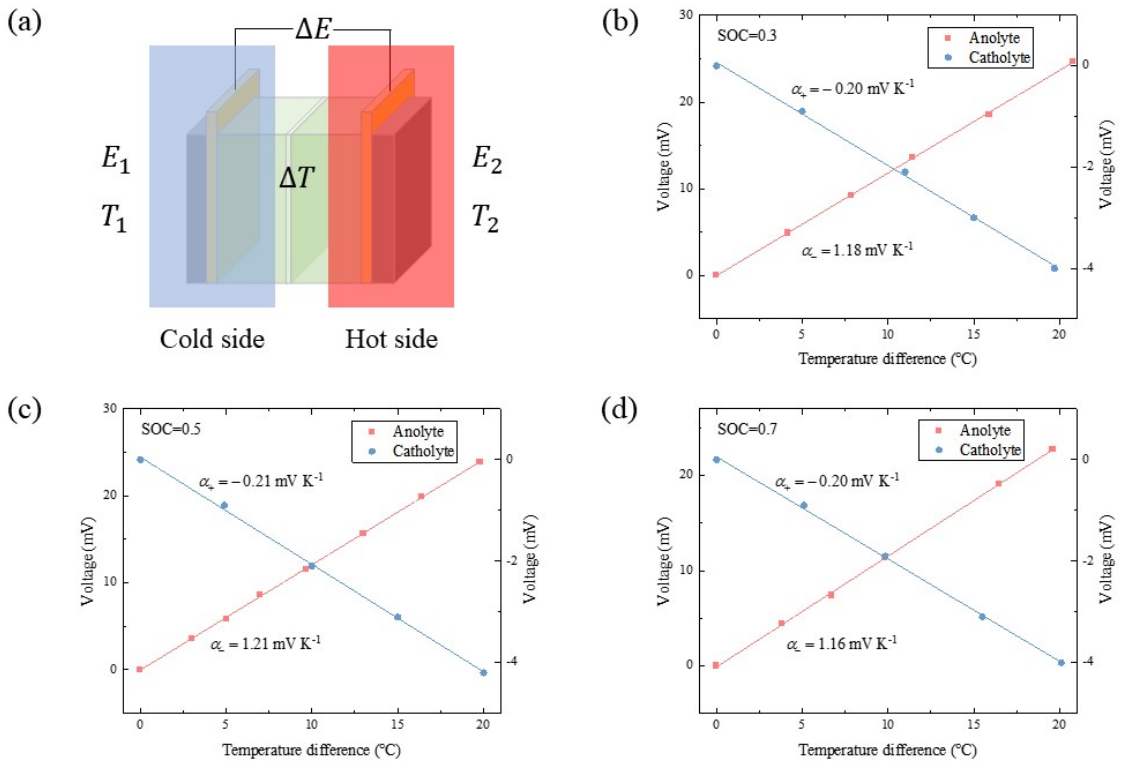

Fig. S3 Measurement of temperature coefficient of half-cell. (a) experimental method for Temperature coefficient of half-cell. (b) Temperature coefficient of half-cell when SOC is 0.3, (c) 0.5, and (d) 0.7

Supplementary Note 6

Experimental system for testing specific heat capacity:

The experimental system is composed of Liquid specific calorimeter, metering pump, back pressure valve, electronic scale and computer, as shown in Fig. S4. The fluid traverses the course delineated in the illustration, exiting the reservoir through metering pump, liquid specific calorimeter, and back pressure valve, before ultimately returning to the reservoir. The metering pump, pivotal for regulating the liquid's flow rate, is procured from Dalian Elite Analytical Instruments Co., Ltd. The liquid specific calorimeter, essential for measuring the temperature change of the liquid and heating power during heating, is supplied by Xi'an Xiaxi Electronic Technology Co., Ltd. Additionally, the back pressure valve, also from Xi'an Xiaxi Electronic Technology Co., Ltd., is instrumental in modulating the liquid's pressure for accurate measurement. An electronic scale is employed to ascertain the precise volume of the liquid under scrutiny. A computer connected to both liquid specific calorimeter and the electronic scale facilitates the acquisition of the requisite measurement data.

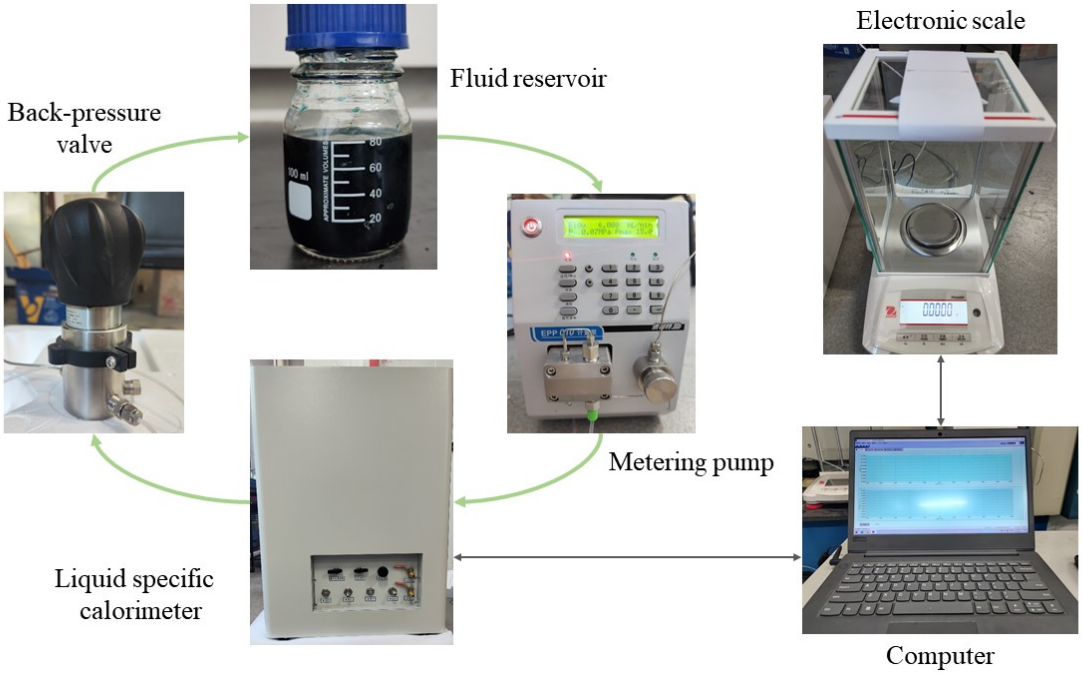

Fig. S4 Experimental system for testing specific heat capacity

The specific experimental operation is as follows:

Connect all the pipes to the instrument, place the liquid inlet pipe below the liquid level of the liquid to be measured, and set the flow rate to 6 mL min^{-1} without additional pressure. Then turn on the metering pump so that the liquid flows along a predetermined route. Then the liquid is heated by the liquid specific calorimeter, and the temperature change of the liquid and heating power are recorded by computer during the heating process. Subsequently, an electronic balance is utilized to gauge the mass of the liquid that has flowed out within a 240-second interval, thereby enabling the computation of the liquid's actual volumetric flow rate. Finally, the heat capacity of the liquid is calculated in the software. The experimental results are shown in the table below.

Table. S4 Specific heat capacity of electrolyte

Liquid name	Test value of specific heat capacity ($J\ g^{-1}K^{-1}$)	Average value of specific heat capacity ($J\ g^{-1}K^{-1}$)	Density ($g\ mL^{-1}$)
Commercial all-vanadium electrolyte	2818.8375 2795.347 2826.6971	2813.6272	1.3174

Supplementary Note 7

Thermal stability of V^{5+}:

Fig. S5 shows the thermal stability of V^{5+} at different temperatures (40°C, 45°C, 50°C and 60°C). At 40°C and 45°C, the 20 mL fully charged anolyte can remain stable without precipitation after two hours. At 50°C, the electrolyte was clarified without precipitation after standing for one hour, while a small amount of precipitation was observed after two hours. At 60°C, the precipitation was observed after standing for one hour, and the precipitation increased significantly after two hours. Therefore, it is concluded that for the commercial vanadium electrolyte with 1.7 M vanadium ion and 4.7 M SO_4^{2-}, the maximum operating temperature should not exceed 45°C. The operating temperature can reach 50°C for short running time and 45°C for long running time. In the actual process, the anolyte and catholyte flow during the charging process, and SOC changes. There will not be a situation where fully charged electrolyte is at high temperature for too long, so the observation results for two hours are valid.

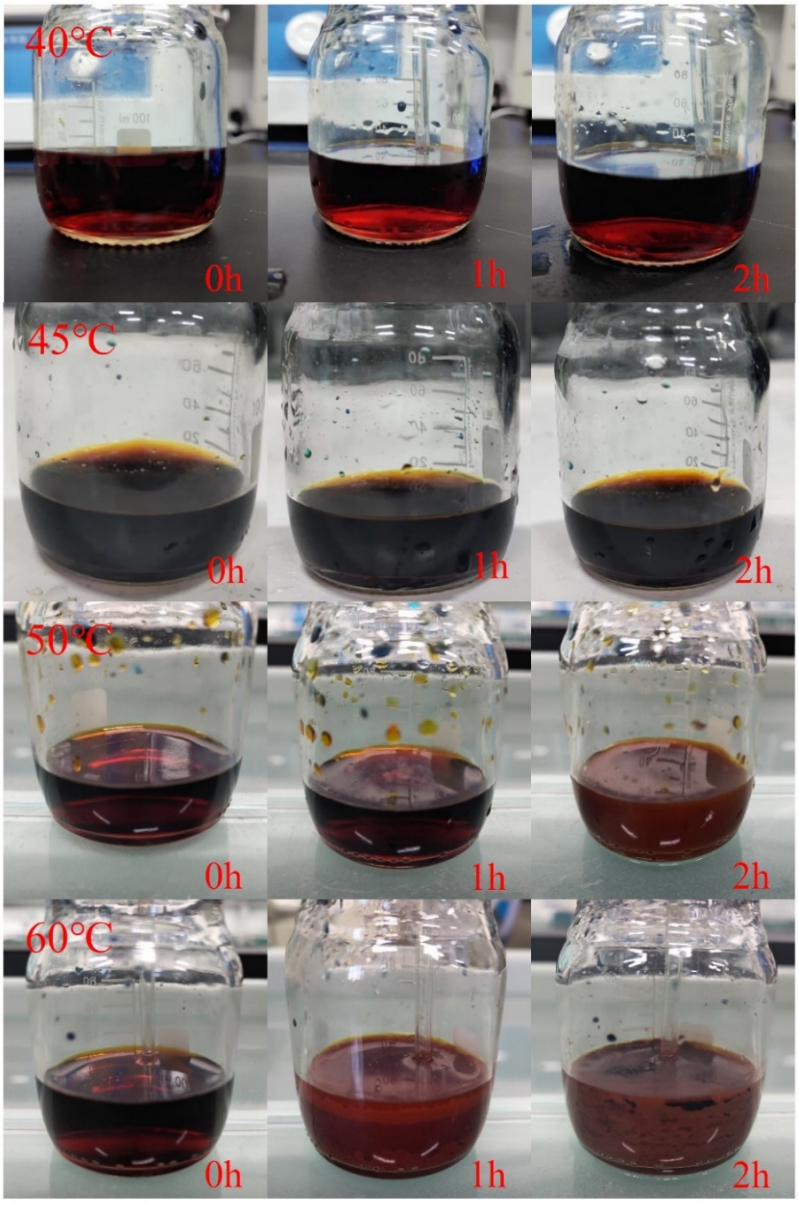

Fig. S5 Thermal stability of V^{5+} at different temperatures

Thermal stability of V^{2+}, V^{3+} and V^{4+}:

Similarly, fully charged anolyte (V^{2+}), anolyte (V^{3+}) and fully discharged catholyte (V^{4+}) are cooled to 0°C and left for two hours, and the change is observed every hour. After two hours, no precipitation was observed in the electrolyte. It is concluded that the commercial vanadium electrolyte is also stable at low temperature.

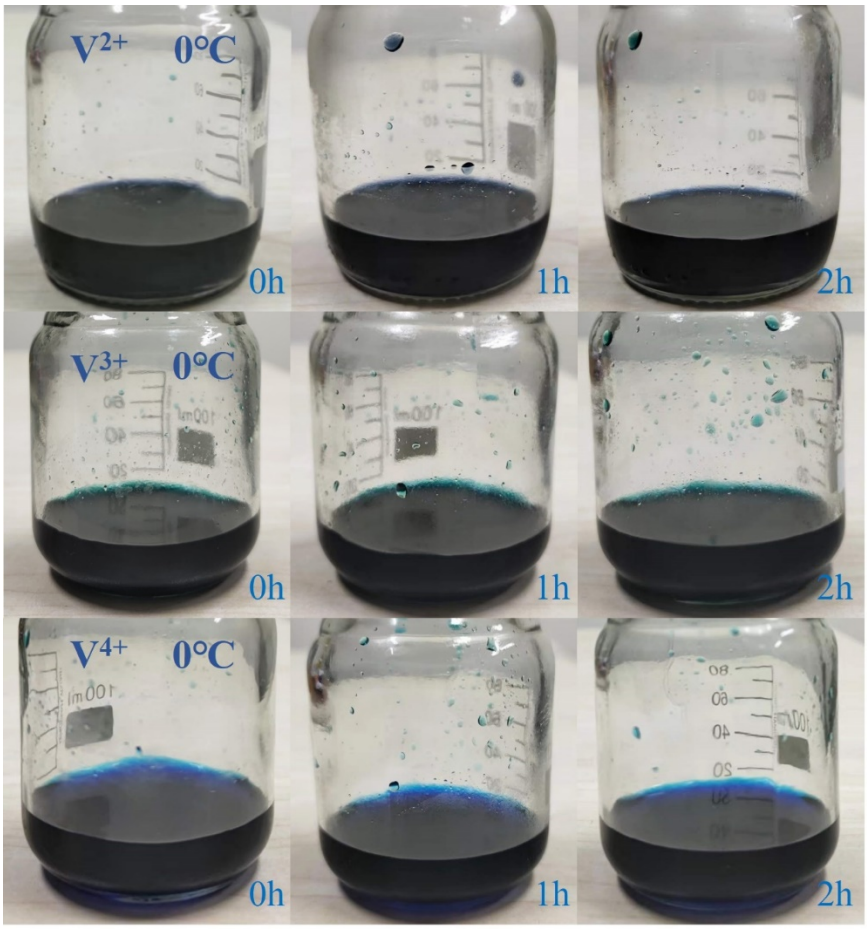

Fig. S6 Thermal stability of V^{2+}, V^{3+} and V^{4+} at different temperatures